HST search for giant planets around white dwarfs in the Hyades

Wolfgang Brandner (MPIA, Heidelberg), Hans Zinnecker (DSI Stuttgart; UAutonoma de Chile), Taisiya Kopytova (DKFZ Heide;berg; Ural Federal Univ., Yekaterinburg)

Abstract

We carried out a deep high-contrast direct imaging search for giant planets around seven single white dwarfs in the nearby (distance ≈45 pc) Hyades open cluster (age ≈625 Myr) using the Hubble Space Telescope and its NICMOS instrument. No planets were found. Compared to a previous search with SPITZER/IRAC using infrared excess in the white dwarfs as an indicator for unresolved very low-mass companions, which derived detection limits of 7 to 11 M_{Jup}, our detection limits for angular separations ≥500mas are considerably lower, i.e. in the range 5 to 7 M_{Jup}. The non-detections are in line with radial velocity studies around K-type giants, which do not find any giant planets around stars more massive than ≈3 solar masses.

Introduction

White dwarfs offer two key advantages compared to main sequence stars in direct imaging searches:

- As the white dwarf progenitors loose about 75% of their initial mass during the Red and Asymptotic Giant Phases (see Table 1), planetary orbits with initial semi-major axis of, e.g., 5 A.U. expand to 20 A.U., hence making them easier to resolve (Table 2, bottom, see also Wolthoff, 2016, and references therein, in particular Villaver & Livio, 2009).
- Due to their small diameter, white dwarfs have a significantly lower luminosity than main sequence stars, hence making the contrast problem less severe.

Table 1. Basic astrophysical parameters of the Hyades single white dwarfs and date of HST/NICMOS observations

name	alt. name	J [mag]	H [mag]	distance [pc]	M_{init} [$M_\odot$]	M_{final} [$M_\odot$]	obs. date
WD0352+096	HZ 4	14.83±0.04	14.87±0.06	35.0	3.59	0.80	2003-11-04
WD0406+169	LB 227	15.70±0.07	15.47±0.12	50.2	3.49	0.85	2004-02-07
WD0421+162	VR 7, LP 415-46	14.75±0.04	14.82±0.06	45.0	2.90	0.70	2004-02-15
WD0425+168	VR 16, LP 415-415	14.63±0.03	14.65±0.05	47.9	2.79	0.71	2003-11-05
WD0431+126	HZ 7	14.77±0.03	14.80±0.06	47.3	2.84	0.69	2003-11-06
WD0437+138	LP 475-242	15.32±0.05	15.51±0.12	46.0	3.41	0.74	2003-11-07
WD0438+108	HZ 14	14.50±0.04	14.62±0.05	49.4	2.78	0.73	2003-11-09

Notes: apparent magnitudes are from 2MASS; distances are based on GAIA DR2 parallaxes (Gaia Collaboration et al. (2016, 2018); Bailer-Jones et al. (2018)), which within the uncertainties are in very good agreement with the distances previously reported by Schilbach & Röser (2012); initial and final mass estimates are from Kalirai et al. (2014)

The larger angular separation and reduced contrast requirements make direct imaging searches for planetary companions around white dwarfs promising. At an age of ≈625 Myr for the Hyades cluster, giant planets are still relatively warm, and hence self-luminous in the near infrared.

Observing set-up

The observations (see Table 1) were carried out with NIC1 for two HST roll angles separated by 20 deg. The two roll angles facilitate improved point spread function subtraction via angular differential imaging (see Müller & Weigelt 1987). Each white dwarf was observed in F110W (1 orbit) and F160W (2 orbits). The observations were furthermore obtained in a 2-point dither pattern was applied for better dark and background subtraction.

Results

Figure 1 shows the residual PSF images of the seven white dwarfs in the F110W filter, and a simulated planet at an angular separation of 500 mas, and 7.0 mag fainter than the host star. No companion to any of the white dwarfs could be identified at separations larger than 500 mas, corresponding to initial semimajor axis in the range 4 to 6.5 A.U.

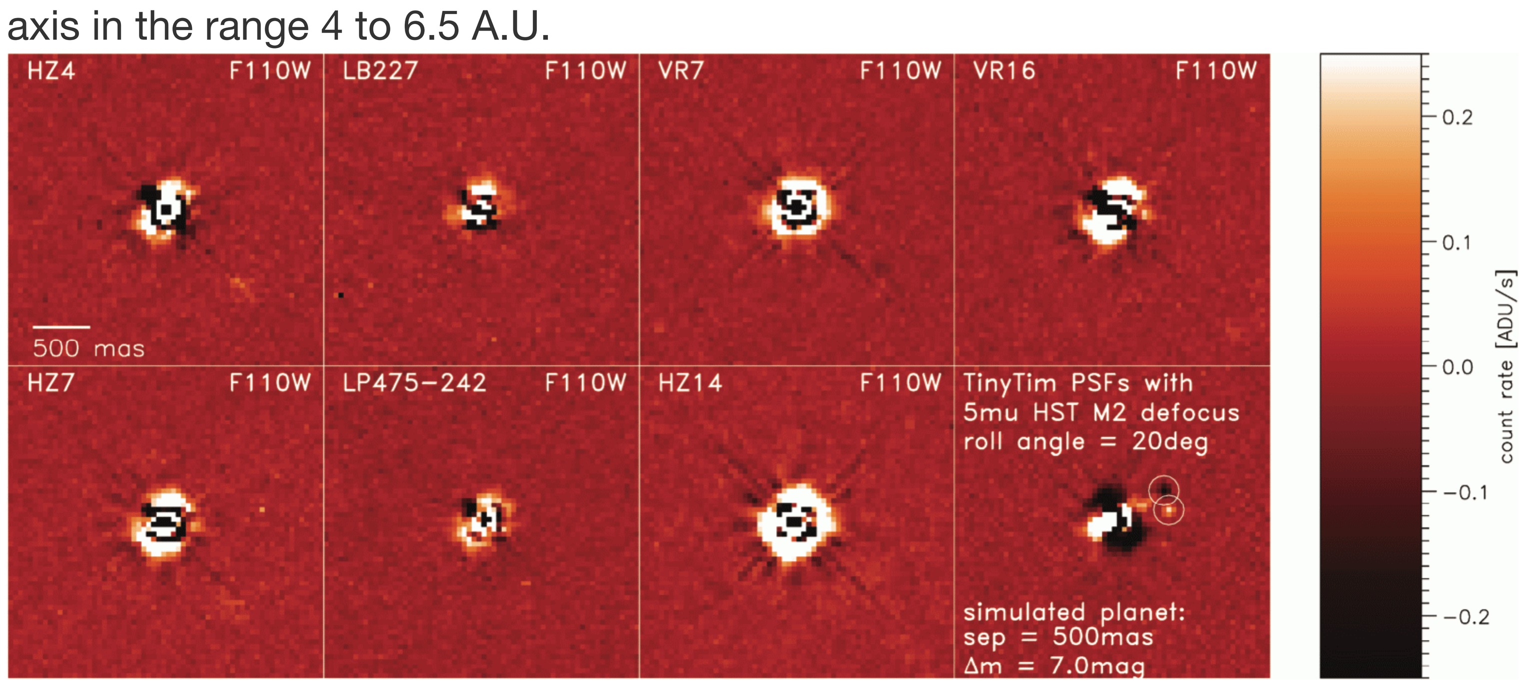

Figure 1: Roll subtracted residual PSF images of the seven white dwarfs (left to right, top to bottom) and of a simulated exoplanet (lower right) in F110W

Figure 2 visualizes the depth of search of the HST/NICMOS study according to the models by Baraffe et al. (2003). The detection probabilities take into account random orientation and phase of the potential orbits for a fixed orbital eccentricty of 0.35 (corresponding to the mean eccentricity of confirmed exoplanets with semimajor axis between 4 and 20 A.U.). For initial semimajor axes ≥6 A.U., we derive lower detection limits of 5 to 7 M_{Jup} (Brandner et al. 2021) than a previous SPITZER/IRAC study, which surveyed for infrared excess in the unresolved white dwarfs (Farihi et al. 2008).

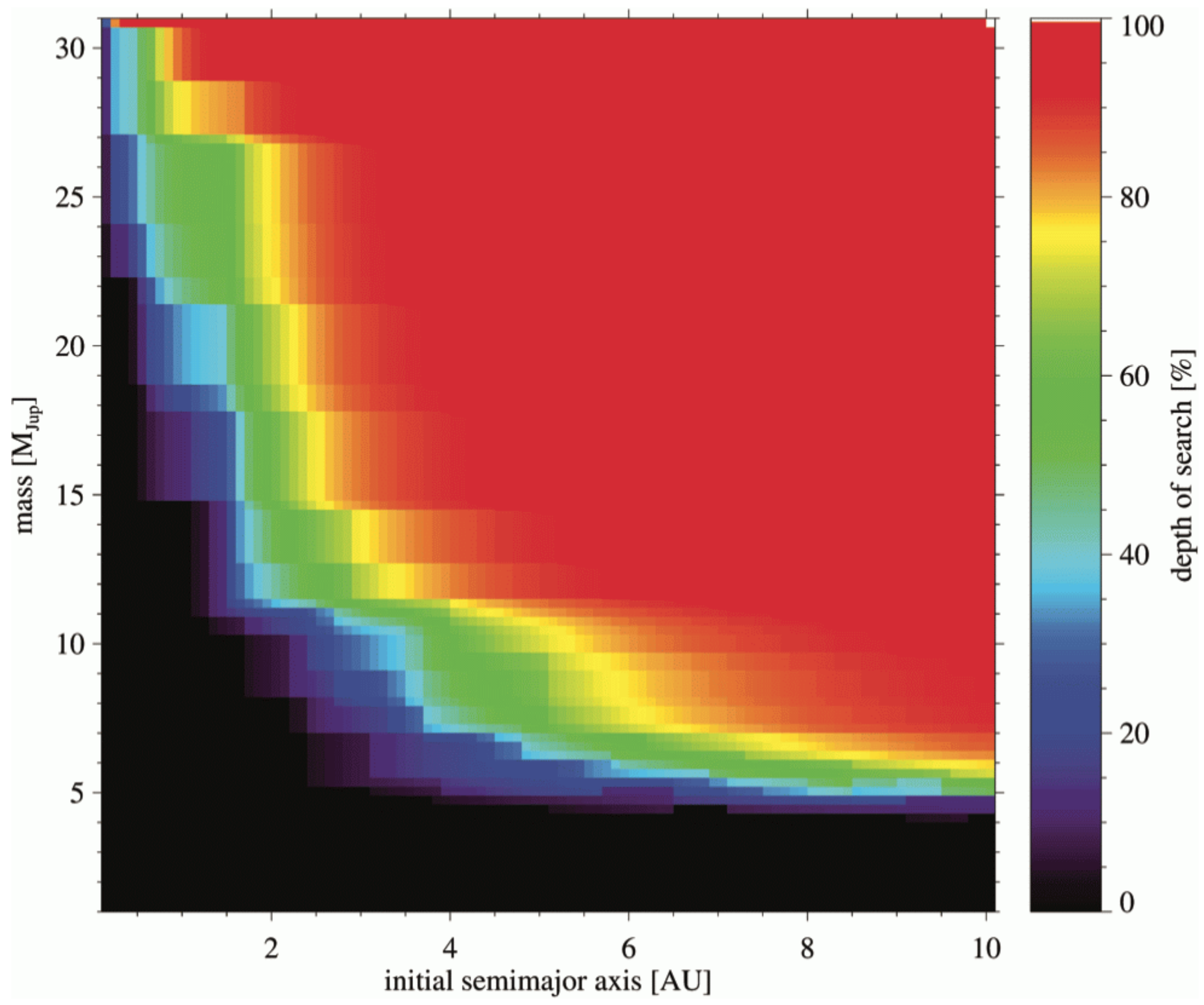

Figure 2: Depth of search, visualizing the probability for detecting a substellar companion to our sample of seven white dwarfs as a function of initial semimajor axis and mass.

Table 2. Detection limits at angular separation ≥ 0.5″ in F110W and F160W: brightness difference, 3σ apparent and absolute magnitude limit, corresponding upper mass limit for substellar companions according to evolutionary and atmospheric models, and current and initial projected physical separation corresponding to 0.5″ based on mass-loss estimates for the white dwarf progenitors and assuming a typical orbital eccentricity of 0.35. Mass limits at 4.5 μm are from Farihi et al. (2008) and are based on Baraffe models.

name: WD...	0352+096	0406+169	0421+162	0425+168	0431+126	0437+138	0438+108
Δm_{F110W} [mag]	8.48	7.79	8.60	8.59	8.62	8.35	8.39
$m_{limF110W}$ [mag]	23.31	23.49	23.35	23.22	23.39	23.67	22.89
$M_{limF110W}$ [mag]	20.6	20.0	20.1	19.8	20.0	20.4	19.4
$mass_{Baraffe}$ [$M_{Jupiter}$]	4.6	5.7	5.5	6.2	5.7	4.9	6.7
$mass_{hothycl}$ [$M_{Jupiter}$]	7.7	8.6	8.5	9.0	8.6	8.0	9.6
$mass_{coldhycl}$ [$M_{Jupiter}$]	9.1	10.3:	10.1:	10.8:	10.3:	9.5	11.7:
Δm_{F160W} [mag]	7.74	6.70	7.50	7.80	7.65	7.35	7.63
$m_{limF160W}$ [mag]	22.61	22.18	22.31	22.45	22.46	22.86	22.26
$M_{limF160W}$ [mag]	19.9	18.7	19.0	19.0	19.1	19.5	18.8
$mass_{Baraffe}$ [$M_{Jupiter}$]	5.9	8.2	7.2	7.2	7.0	6.5	7.8
$mass_{hothycl}$ [$M_{Jupiter}$]	8.3	10.0	9.5	9.5	9.4	8.8	9.8
$mass_{coldhycl}$ [$M_{Jupiter}$]	9.8	12.1:	11.5:	11.5:	11.3:	10.5:	11.9:
$mass_{4.5\mu m}$ [$M_{Jupiter}$]	10	7	10	10	10	8	11
a_{curr} [A.U.]	21	30	27	29	28	28	30
a_{init} [A.U.]	4.7	7.4	6.5	7.3	6.9	6.0	7.8

Notes: we selected models for solar metallicity by Baraffe et al. (2003) and Spiegel & Burrows (2012). In the latter case, the mass estimates are based on models assuming hybrid clouds and either a hot (hothycl) or a cold (coldhycl) start.
":" indicates that the mass limits are based on extrapolation beyond the mass range covered by the models.

Discussion and Outlook

The non-detection is in line with radial velocity studies of K-giants (Reffert et al. 2015), which do not find planetary mass companions to stars more massive than ≈3 solar masses. Potential explanations are that the initially dense cluster environment inhibits/hinders the formation of massive giant planets, or that the energetic radiation of the host stars themselves has an effect on dust growth and gas evaporation, and hence the planet formation efficiency. JWST observations should ultimately expand detection limits to the sub-Jupiter mass regime.

References

Bailer-Jones, C. et al. AJ 156, 58 (2018), ADS
Baraffe, I. et al. A&A 402, 701 (2003), ADS
Brandner, W. et al. MNRAS 500, 3920 (2021), ADS
Farihi, J. et al. ApJ 681, 147 (2008), ADS
Gaia Collaboration et al. A&A 595, 1 (2016), ADS
Gaia Collaboration et al. A&A 616, 1 (2018), ADS
Kalirai, J. et al. ApJ 782, 17 (2014), ADS
Müller, M., Weigelt, G. A&A 175, 312 (1987), ADS
Reffert, S. et al. A&A 574, 116 (2015), ADS
Schilbach, E., Röser, S., A&A 537, 129 (2012), ADS
Spiegel, D., Burrows, A., ApJ 745, 174 (2012), ADS
Villaver, E., Livio, M., ApJ 705, 81 (2009), ADS
Wolthoff, V., Evolution of Planetary Systems on the Giant Branch, Master thesis, University of Heidelberg (2016)